View Article Online / Journal Homepage / Table of Contents for this issue
Dynamic Article Links

Soft Matter

Cite this: *Soft Matter*, 2012, **8**, 5477

www.rsc.org/softmatter

**PAPER**

# Designing dynamic surfaces for regulation of biological responses†

**Ji-Hun Seo,[ad] Sachiro Kakinoki,[bd] Yuuki Inoue,[cd] Tetsuji Yamaoka,[bd] Kazuhiko Ishihara[cd] and Nobuhiko Yui*[ad]**

***Received 12th February 2012, Accepted 5th March 2012***
**DOI: 10.1039/c2sm25318f**



ABA block copolymers composed of highly methylated polyrotaxane and hydrophobic anchoring terminal segments containing 2-methacryloyloxyethyl phosphorylcholine (MPC) and *n*-butyl methacrylate (PMB) (OMe-PRX-PMB) were synthesized as a platform of molecularly dynamic biomaterials. A contact angle measurement indicated that polymer surfaces with higher molecular mobility factors ($M_f$) estimated from quartz crystal microbalance with dissipation (QCM-D) measurements showed more significant changes in hydrophilicity in response to an environmental change between air and water; the OMe-PRX-PMB surface showed the highest $M_f$ among the prepared polymer surfaces. Fibrinogen adsorption and its conformational analysis estimated by QCM-D and enzyme-linked immunosorbent assay revealed that large amounts of fibrinogen adsorption occurred in a soft manner on the OMe-PRX-PMB surface and that the antibody binding to the C-terminus of the fibrinogen γ chains responsible for platelet adhesion and activation decreased as the $M_f$ value increased. Furthermore, it was found that the OMe-PRX-PMB surface showed low platelet adhesion and high fibroblast adhesion, suggesting that molecular movement on biomaterial surfaces could be one of the key parameters in the regulation of a non-specific biological response.

## 1. Introduction

When artificial materials are placed in a biological environment, protein–material interaction primarily occurs on the surfaces along with the physicochemical properties of materials.[1–3] The state of adsorbed proteins plays a dominant role in most non-specific biological responses such as foreign body reaction or clot formation.[4] Therefore, the development of anti-fouling materials that are able to prevent non-specific protein interaction has been a critical issue in the field of biomaterials for the last several decades.[5] Although several applications of anti-fouling materials have been reported for the limited number of available biomaterials such as artificial blood vessels, anti-fouling properties also prevent the promotion of tissue regeneration on the materials implanted in a damaged body. Because the extracellular matrix composed of protein molecules is an essential factor for cell adhesion and tissue formation, protein adsorption on the biomaterials is a fundamental requirement.[6] However, non-specifically adsorbed surface proteins also can trigger undesirable biological reactions as mentioned above. This paradoxical problem of protein adsorption has been a fundamental barrier to the development of ideal biomaterials that prohibit non-specific biological reactions as well as promote specific cell adhesion. Because conformational change of adsorbed proteins is the cause of most biological responses on the artificial materials, it is important to regulate protein conformation in the design of ideal biomaterials. A number of variables that have an effect on the conformational change of adsorbed proteins have been reported in the last several decades. These include polarity, charge density, and other geometrical factors such as surface roughness.[7–9] Nowadays, these factors are commonly used to regulate biological responses on artificial materials. However, to the best of our knowledge, there have been no reports on key variables responsible for moderate conformational change that can modulate cell adhesion for tissue regeneration and prevent undesirable foreign body reactions such as blood clotting and inflammatory reaction. Not only dynamic cell membranes but also single protein molecules continuously move on the surface of artificial materials until they determine the thermodynamic standpoint for final conformations.[10] Therefore, even well-defined artificial materials with determined surface properties could not withstand the dynamic responses of the biological environment. We presume that rigid material surfaces with a determined surface nature generate conformational changes in adsorbed proteins, and finally trigger undesirable biological responses. Therefore, in this paper, we present a novel concept, which proposes that dynamic material surfaces that flexibly respond to a dynamic biological environment can possibly overcome the limitations of traditional biomaterials.

[a]*Institute of Biomaterials and Bioengineering, Tokyo Medical and Dental University, Tokyo 101-0062, Japan. E-mail: yui.org@tmd.ac.jp; Fax: +81-3-5280-8027; Tel: +81-3-5280-8020*
[b]*Department of Biomedical Engineering, National Cerebral and Cardiovascular Center Research Institute, Suita, Osaka, 565-8565, Japan*
[c]*Department of Materials Engineering, The University of Tokyo, Tokyo 113-8656, Japan*
[d]*JST-CREST, Tokyo 102-0076, Japan*

† Electronic supplementary information (ESI) available: NMR and AFM images. See DOI: 10.1039/c2sm25318f

Polyrotaxane (PRX) is a representative molecular assembly consisting of a host molecule, *e.g.*, α-cyclodextrin (α-CD), threading a guest molecule, *e.g.*, linear polyethylene glycol (PEG). Because both components are not covalently connected, the threaded α-CD molecules are anticipated to be movable along the PEG backbone. Based on this perspective, we have systematically studied the effect of the molecular mobility of polyrotaxanes on biological interaction with proteins. Throughout these studies, we clarified that CD mobility is influential in enhancing multivalent interaction with receptor proteins in biological ligand-immobilized polyrotaxanes.[11–15] Furthermore, we have demonstrated that cytocleavable polyrotaxanes are very effective in DNA delivery to the nucleus in a target cell.[16–21] As polymeric materials for designing movable surfaces using a polyrotaxane structure, the block copolymer containing the PRX segment was previously synthesized by using an atom transfer radical polymerization method with hydrophobic isobutyl methacrylate.[22] The prepared surface showed high molecular mobility and eliminated adsorption of human plasma fibrinogen by introducing a low degree of methoxy (OMe) groups of α-CD molecules on the PRX segment. In this study, we introduced bio-inert poly((2-methacryloyloxyethyl phosphorylcholine)-co-(*n*-butyl methacrylate)) (PMB) anchoring terminals at both ends of the PRX segment by using the reversible addition-fragmentation chain transfer (RAFT) polymerization method. Furthermore, a higher degree of OMe groups were introduced to each threaded α-CD molecule to modulate the protein interaction on the hydrophilic PRX moiety. The aim of this study is to investigate the dynamic interaction of mobile OMe groups with protein molecules and the associated biological responses including platelet and fibroblast adhesion.

## 2. Materials and methods

### 2.1 Materials

A 2-methacryloyloxyethyl phosphorylcholine (MPC) was obtained from NOF Co. (Tokyo, Japan). 4-(Benzodithioyl)-4-cyanopentanoic acid (CTA) was synthesized according to a previously reported method.[23] α-CD, BMA, sodium hydride, iodomethane, α,α′-azobisisobutyronitrile (AIBN), and all the organic solvents were purchased from Tokyo Kasei Co. (Tokyo, Japan) and used as received. PEG (number average molecular weight of 20 kDa) (PEG 20k) was purchased from the Sigma-Aldrich Chemical Co. (St. Louis, MO, USA), and the hydroxyl end groups were converted to amine groups by using a previously reported method.[24]

Goat polyclonal antibody to mouse IgG conjugated with horseradish peroxidase (HRP) and anti-fibrinogen alpha antibody (49D2) were purchased from Abcam Inc. (Cambridge, MA, USA), and anti-fibrinogen gamma antibody (clone2 G2. H9) was purchased from Millipore (Bedford, MA, USA). Human plasma fibrinogen was purchased from Sigma-Aldrich (St. Louis, MO, USA) and other biological reagents were purchased from Gibco Invitrogen Corp. (Grand Island, NY, USA).

Fresh blood was donated by a healthy human volunteer at the National Cerebral and Cardiovascular Center Research Institute. The whole blood was collected with 10 v/v% of 3.8% trisodium citrate solution, and platelet-rich plasma (PRP) was prepared *via* a centrifugation process (200 gravity, 15 min at 25 °C). After this, the PRP was further centrifuged (1500 gravity, 10 min at 25 °C) to obtain platelet-poor plasma (PPP). The number of platelets in the PRP was then adjusted by PPP to $1.0 \times 10^7$ mL$^{-1}$. The use of whole blood and platelets were approved by the Biosafety Committee at National Cerebral and Cardiovascular Center Research Institute.

### 2.2 Block copolymer synthesis

**Synthesis of pseudo-PRX macro CTA.** Previously, PEG 20k macro chain transfer agent (CTA) was synthesized as follows: 1 g of PEG 20k bis-amine (0.050 mmol), and 0.018 g of dimethylamino pyridine (0.15 mmol) were dissolved in 5 mL of dichloromethane. To this, 0.14 g of CTA (0.50 mmol) and 0.082 g of water soluble carbodiimide (0.50 mmol) were added and stirred for 12 h at room temperature. Next, some fresh dichloromethane was added and the mixture was re-precipitated in cold diethyl ether. The crude product was then dissolved in water, and the dialysis process was carried out (MWCO 3500) for a day, followed by the lyophilization process.

The obtained PEG macro-CTA (0.35 g) was then mixed with 3.5 g of α-CD in 25 mL of water at room temperature until the light-pink and turbid inclusion complex was formed. The precipitate was then isolated by means of the centrifuge process, and washed again with 25 mL of water, followed by a repeat of the centrifugation process. The precipitate was then freeze-dried to obtain pink-colored inclusion complex of pseudo-PRX macro CTA.

**Synthesis of PRX-PMB block copolymer.** A 0.600 g of pseudo-PRX macro-CTA was allowed to react with 0.354 g of MPC (1.20 mmol) and 0.633 g of BMA (4.45 mmol) monomer in 7 mL of ethanol–toluene (1 : 1) mixed solvent, by using 0.820 mg of AIBN (5.00 μmol) as an initiator. The heterogeneous solution was bubbled with an Ar atmosphere for 15 min prior to placement in a 60 °C oil bath. After 24 h, 15 mL of fresh mixed solvent was added to the solution and the precipitate was obtained by means of the centrifugation process. The obtained polymer was sequentially washed with ethanol, acetone, dimethyl sulfoxide (DMSO), and acetone to remove residual monomers and α-CD. The final precipitate was then dried at 40 °C *in vacuo* and the polymer was obtained as a white powder. A similar process was carried out to synthesize PMB and PEG-PMB by using CAT or PEG-CTA as a macro CTA.

**Methylation of PRX-PMB block copolymer.** 200 mg of the synthesized PRX-PMB block copolymer was heterogeneously dissolved in 7 mL of dehydrated DMSO. To this, 0.155 g of sodium hydride (6.3 mmol) was added under an Ar atmosphere and mixed for 30 min at room temperature. Next, 0.102 g of iodomethane (0.719 mmol) was slowly injected to the mixture and stirred for 3 h at room temperature. After the pH was neutralized with 6 N HCl solution, the mixture was transferred to a dialysis tube (MWCO0 : 20000) and the dialysis process was carried out for 3 days. The methylated PRX-PMB (OMe-PRX-PMB) block copolymer was then obtained by means of the lyophilization process.

### 2.3 Surface characteristics

The synthesized polymer (5 mg) was initially dispensed in 5 mL ethanol. After that, 5 mL of water was added to prepare 0.05 wt % of clear polymer solution. Each polymer solution (30 μL) was then uniformly cast on a Cell Desk™ (Sumitomo Bakelite Co., Japan), and dried in a clean box at room temperature for a day. Each polymer surface was stabilized in water for a day prior to the surface characterization and other biological evaluations.

X-ray photoelectron spectroscopy (XPS) was used to analyze the surface chemical elements by using a magnesium $K_\alpha$ source with a take-off angle of 90° (Kratos/Shimadzu, Kyoto, Japan). The characterized elements were C, N, and P and the binding energies were referenced to the $C_{1s}$ peak at 285.0 eV.

The static water and air bubble contact angles were measured using a goniometer (Kyowa Interface Science Co., Tokyo, Japan). Prior to the measurement, the surface tension of water (72 mN $m^{-1}$) was confirmed by means of the pendant drop method using a Young–Laplace curve-fitting algorithm. Under dry conditions, 3 μL of water droplets were brought in contact with the polymer surface for 30 s, and the contact angles were measured using photographic images. Under wet conditions, 5 μL of air bubble was brought in contact with the surfaces in water, and the contact angles again were measured using photographic images.

Quartz crystal microbalance with dissipation (QCM-D) monitoring of the polymer surfaces was carried out by using Q-sense E1-HO (Meiwafosis Co., LTD, Tokyo, Japan). The molecular mobility at the hydrated surfaces was estimated as follows: the Au sensor was cleaned by applying an $O_2$ plasma treatment for 5 min and a sequential washing with acetone and ethanol, and dried with Ar blowing. The sensor was placed in an open-type chamber equipped with the QCM-D apparatus at 25 °C. The resonance frequency at 35 MHz ($f_{gold,\ dry}$) and the dissipation energy ($D_{gold,\ dry}$) was then measured. Subsequently, $f_{gold,\ wet}$ and $D_{gold,\ wet}$ in a hydrated state were measured with the bare gold in contact with pure water. After the water was removed from each polymer solution and dried by using a stream of air, 20 mL of it was dropped on the surface. After the surface was dried, the resonance frequencies ($f_{sample,\ dry}$ and $f_{sample,\ wet}$) and dissipation energies ($D_{sample,\ dry}$ and $D_{sample,\ wet}$) of the coated surface in both the dry and hydrated states were measured using the same procedure as above.[22]

### 2.4 Evaluation of biological responses to the block copolymer surface

**Protein adsorption test.** The polymer-cast Cell Desk™ was immersed in a 0.3 mg $mL^{-1}$ of fibrinogen solution or 10% human plasma in phosphate buffered saline (PBS, pH 7.4) for 1 h at 37 °C. Next, the samples were rinsed twice with 500 mL of fresh PBS employing the stirring method (300 rpm for 5 min). The adsorbed protein was detached in sodium dodecyl sulfate (SDS, 1 wt% in water) by sonication for 20 min, and the protein concentration in the SDS solution was determined by means of the micro-BCA™ method.

The state of adsorbed fibrinogen was also analyzed by QCM-D measurements. The Au substrate was cast with each polymer solution, and the energy dissipation factor ($D$) and frequency ($f$) were stabilized under a flow of PBS (0.1 mL $min^{-1}$). Then, a 0.3 mg $mL^{-1}$ fibrinogen solution was flowed for 1 h, and fresh PBS was flowed for another 1 h. Each $D$ and $f$ value was continuously monitored during the whole process of protein adsorption. The amount of adsorbed proteins was calculated by using the simplified Sauerbrey equation with an overtone value of 7 and C = 17.7 ng $cm^{-2}$, as follows:[25]

$$\Delta m = -C\Delta f/n$$

An enzyme-linked immunosorbent assay (ELISA) was carried out to estimate the conformational change of adsorbed fibrinogen as follows: initially, each polymer surface was brought in contact with whole human plasma for 5 min at 37 °C. After rinsing three times with PBS, each sample was brought in contact with 2 μg $mL^{-1}$ of the primary antibody (anti-fibrinogen alpha or gamma) solution for 1 h at room temperature. After rinsing four times with PBS, samples were allowed to react with 8 μg $mL^{-1}$ of the secondary antibody conjugated with HRP in bovine serum albumin (BSA) pre-treated 24 well plates for 2 h. After rinsing six times with PBS-T, 0.5 mL of solution (mixture of 10 mL guanylic acid buffer (pH 3.3), 0.125 mL of 3,3′,5,5′-tetramethylbenzidine (44 mM), and 0.018 mL of $H_2O_2$) was added to each sample surface in the BSA pre-treated well. After the reaction was quenched with 2 N of sulfuric acid, the absorbance at 450 nm in each resulting solution was measured by a micro plate reader (Multiskan FC, Thermo Fisher Scientific, St. Herblain, France).

Each polymer surface was brought in contact with 500 μL of PRP in a 24 well plate at 37 °C for 2 h. After rinsing three times with fresh PBS, platelet adhesion was quantitatively analyzed by means of lactate dehydrogenase (LDH) assay, and the morphology of adhering platelets was observed using a fluorescent microscope after dying F-actin with rhodamine conjugated phalloidin.[26]

The cell adhesion test using NIH3T3 mouse fibroblast was performed on each polymer surface. Approximately 1.0 × $10^5$ cells in 1.0 mL of minimum essential medium (Invitrogen Corp., Carlsbad, CA, USA) supplemented by 10% fetal bovine serum was incubated on polymer surfaces for 6 h. After rinsing with fresh medium, the surface adhering cells were observed using an optical microscope and the number of adhering cells was counted by a Cell Counting Kit #8 (Dojindo, Tokyo, Japan).

## 3. Results and discussion

### 3.1 Preparation of PRX block copolymers

Scheme 1 shows the overall concept of this study in preparing molecularly dynamic surfaces for evaluating biological

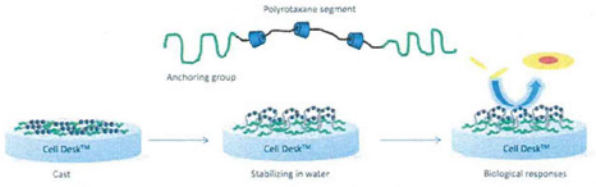


**Scheme 1** Schematic explanation of development of dynamic surface.

responses. To develop dynamic surfaces, PRX segments are necessary to be combined with hydrophobic anchoring terminal segments at both ends. Here, a random copolymer segment composed of MPC and BMA (PMB) was selected as an anchoring terminal (Fig. 1). The PMB segment is a well-known coating unit that can be stably immobilized on a hydrophobic material's surface to prevent non-specific biological responses.[27] To synthesize the PRX block copolymer, RAFT chain transfer agent (CTA) was initially introduced to PEG-bisamine, and pseudo-PRX macro CTA was synthesized with α-CD. Subsequently, MPC and BMA were introduced *via* the RAFT polymerization method. Then, the hydrophobic OMe group was introduced to each hydroxyl group of the α-CD molecules. As a result, around 90% of the hydroxyl groups were successfully substituted by OMe groups. Fig. 2 shows the $^1$H-NMR and FT-IR results of the synthesized OMe-PRX-PMB. Obviously, a strong OMe peak was observed at 3.2 and 3.3 ppm, which does not exist in PRX-PMB (Figure S3†). All the functional groups containing MPC units were successfully confirmed by combination of $^1$H-NMR and FT-IR results. The detailed molecular profiles are summarized in Table 1.

### 3.2 Surface characterization of PRX block copolymer

The prepared polymer surfaces cast on the Cell Desk™ were analyzed by XPS. In all the cases of polymer surfaces, characteristic $N_{1s}$ and $P_{2p}$ signals from the PMB segment appeared at 402.5 eV and 134.0 eV, respectively, whereas the characteristic peak of the Cell Desk™ surface at 290 eV $C_{1s}$ had disappeared (Fig. 3). This result indicates that all the polymer samples are uniformly prepared on the Cell Desk™ surface by means of the simple solvent cast method. Throughout an ellipsometry measurement, it was confirmed that all the polymer films were formed within a thickness of 20∼30 nm (data not shown). In any case, it was confirmed that all the polymers were stably cast on the overall Cell Desk™ surface by anchoring the PMB segment.

The wettability of the prepared polymer surfaces was estimated in both air and water using water droplets and air bubbles, respectively. The contact angles of the air bubbles on the PMB, PRX-PMB, and OMe-PRX-PMB surfaces were not measured, because the air bubbles were rolling on these surfaces. These findings indicate that the surfaces are extremely hydrophilic in an aqueous environment and the contact angles are close to 0°. The contact angle hysteresis along with an air–water environmental change was indirectly measured by comparing both results (Fig. 4). The PMB surface showed a slightly higher contact angle hysteresis (∼40°) than that of the Cell Desk™, which is possibly due to the increased directionality of the hydrophilic phosphorylcholine group in the water compared to the state in the air as previously reported.[28] The PEG-PMB and PRX-PMB surfaces showed a contact angle hysteresis of around 60°. It is thought that the swelling of the hydrophilic PEG and PRX segments of the block copolymer in the water was contributing to the slight increase of the contact angle hysteresis in addition to the directionality effect of the PMB segment. In contrast to the moderate hysteresis changes in these control samples, the OMe-PRX-PMB surface showed a contact angle hysteresis of around 100°. This indicates that the surface property of the OMe-PRX-PMB has drastically changed in response to the environmental change between air and water. The smoothness of all the surfaces was confirmed by atomic force microscope measurement, suggesting that the effect of surface roughness on the contact angle hysteresis should be negligible (Figure S4†). Even though more supporting information is required, we speculate that this dynamic change in the surface property is due to the dynamic movement of CD molecules on the PEG backbone.

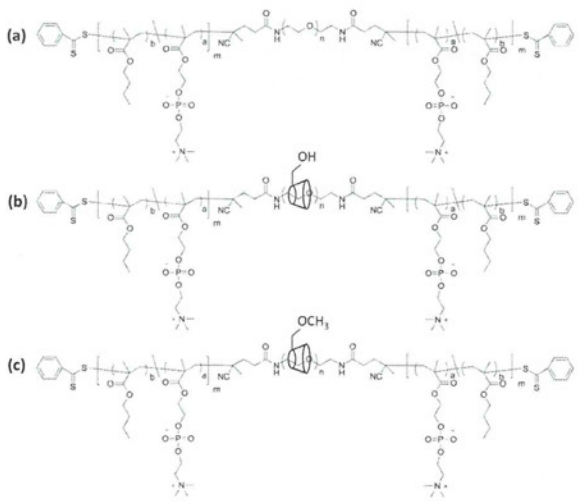


**Fig. 1** Molecular structure of (a) PEG-PMB, (b) PRX-PMB, and (c) OMe-PRX-PMB.

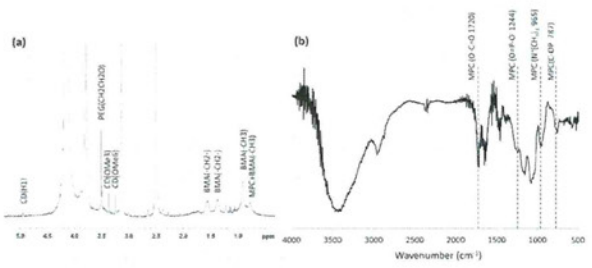


**Fig. 2** (a) $^1$H NMR (DMSO-$d_6$:MeOD = 1 : 1) and (b) FT-IR spectra of OMe-PRX-PMB.

To estimate the dynamic nature of the prepared PRX block copolymers in more detail, the surface dynamics in an aqueous media were estimated by the QCM-D measurement method as previously reported.[22] Generally, the energy dissipation value on a materials surface ($\Delta D$) is directly related to the viscoelasticity of the materials adsorbed on an Au surface. When highly mobile surface elements such as tethering polymer chains or weakly cross-linked hydrogels exist, $\Delta D$ values drastically increase against rigid surfaces. This viscoelasticity of the surface could be interpreted as one of the parameters that indicate dynamic molecular movement of the surfaces. To consider the effect of the amount of polymers, each $\Delta D$ value was normalized to its adsorption mass related factor ($\Delta f$) using the following equation:

$$\text{Surface mobility factor } (M_f) = (D_{\text{sample, wet}} - D_{\text{gold, wet}})/(f_{\text{gold, dry}} - f_{\text{sample, dry}})$$

**Table 1** Molecular profile of the synthesized polymers ($^1$H NMR)

| | MPC (mol% in PMB) | BMA (mol% in PMB) | PEG (weight %) | Number of CD per PEG chain |
|---|---|---|---|---|
| Cell Desk™ | 0 | 0 | 0 | 0 |
| PMB | 19 | 81 | 0 | 0 |
| PEG-PMB | 23 | 77 | 24 | 0 |
| PRX-PMB | 12 | 88 | 23 | 12 |
| OMe-PRX-PMB | 12 | 88 | 23 | 12<br>methylation >90% |

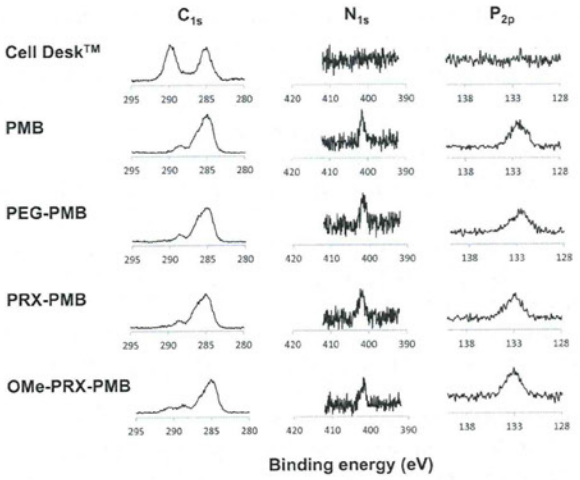


**Fig. 3** XPS profile of cast polymer surfaces.

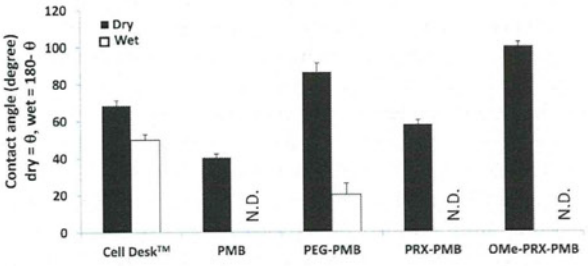


**Fig. 4** Contact angles measured by water droplet in air and air bubble in water (n = 3).

Fig. 5 (a) shows the resulting value of $M_f$ on each prepared polymer surface. The PEG-PMB showed a slightly higher $M_f$ value than PMB. This is possibly due to the chain mobility of the hydrated loop-type PEG segment in the middle of the block copolymer. The OMe-PRX-PMB surface showed the highest $M_f$ value among the prepared polymer surfaces, suggesting that the OMe group-containing the PRX segment exhibits the highest molecular mobility in an aqueous media. The lower $M_f$ value on the PRX-PMB surface compared to those on the PEG-PMB and OMe-PRX-PMB surfaces is thought to be caused by the rigid crystalline formation of the CD molecules by intermolecular hydrogen bonding that interferes with the mobility of the PEG backbone. In any event, it was confirmed that the OMe-PRX-PMB surface exhibits the highest surface viscoelasticity—possibly induced by the dynamic molecular mobility on the surface—compared to other control polymer surfaces. Of special interest is the plot of the contact angle hysteresis along with the $M_f$ value (Fig. 5 (b)). It is obvious that the relationship between the contact angle hysteresis and the $M_f$ value is straightforward. This finding suggests that the dynamic change of surface wettability in response to the environmental change, is strongly governed by the molecular mobility on the surface.

### 3.3 Non-specific protein interaction with PRX block copolymer surfaces

Fig. 6 (a) shows the result of the human fibrinogen adsorption test. As expected, hydrophilic control samples (PMB, PEG-PMB, and PRX-PMB surfaces) showed relatively low fibrinogen adsorption. Similar results were also confirmed in the case of the

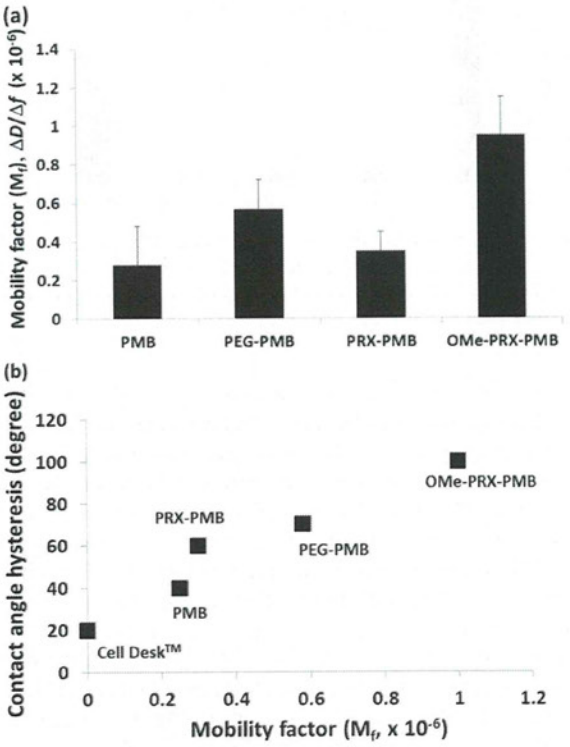


**Fig. 5** (a) Result of $M_f$ estimated from QCM-D and (b) plot of contact angle hysteresis *versus* $M_f$ values (n = 3). The contact angle hysteresis was calculated by subtracting the contact angle of the water droplet in the air from that of the air bubble in the water bubble in water (n = 3).

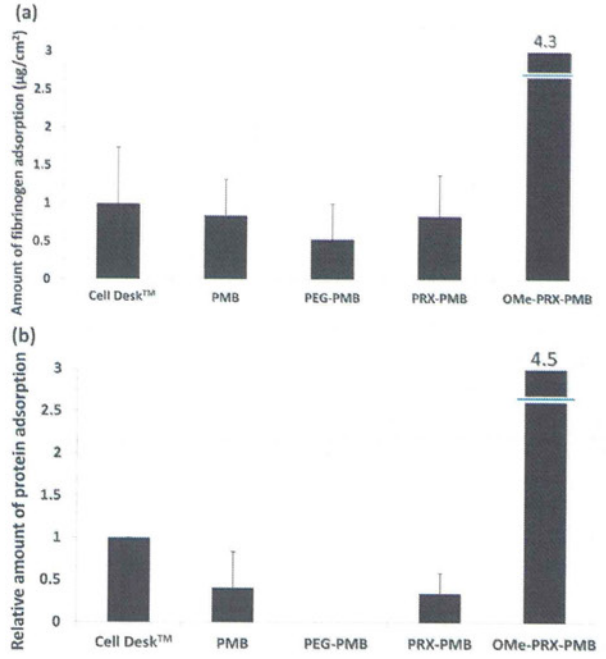


**Fig. 6** Protein adsorption measured by micro-BCA™ method using (a) human fibrinogen at 10% plasma concentration and (b) 10% human PPP (n = 3).

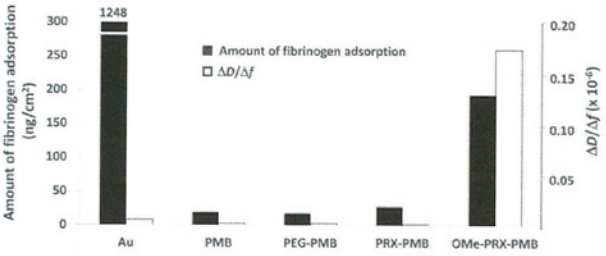


**Fig. 7** Fibrinogen adsorption and $\Delta D/\Delta f$ value measured by QCM-D using 10% plasma concentration of human fibrinogen. Adsorption condition: flow rate = 0.1 mL min$^{-1}$, 1 h protein flow followed by 1 h PBS flow (pH 7.4).

whole human plasma adsorption test (Fig. 6 (b)). These results indicate that non-specific interaction between the hydrophilic control samples and the plasma protein was not very significant. In contrast, a significantly large amount of protein adsorption was observed on the OMe-PRX-PMB surface in both the fibrinogen and whole plasma adsorption test. Because the OMe-PRX-PMB surface exhibited an extremely hydrophilic nature in water (Fig. 4), the surface hydrophilicity in an aqueous environment could not explain this result. Even though the OMe are hydrophobic groups, they along with the rest of the polymer provide adequate enough hydrogen bonding to make the surface appear hydrophilic in aqueous media. However, these OMe groups exposed on the outermost surface still allow for contact with plasma proteins which leads to protein binding and accumulation.

To understand the state of the adsorbed proteins more clearly, fibrinogen adsorption was carried out by means of QCM-D under the flow adsorption condition. As a result, the adsorption behavior similar to that of micro-BCA™ was further confirmed on all the polymer surfaces (Fig. 7). In particular, a significantly large amount of fibrinogen adsorption was observed only on the hydrophobic Au and OMe-PRX-PMB surfaces. However, it is noteworthy that the state of adsorbed fibrinogen was quite different between the bare Au and OMe-PRX-PMB surfaces. In the case of the bare Au surface, the adsorbed fibrinogen molecules showed a very low $\Delta D/\Delta f$ value, which indicates that the state of the adsorbed fibrinogen molecules is very rigid because the interaction with the Au surface is quite strong. In contrast, the adsorbed fibrinogen on the OMe-PRX-PMB surface showed a significantly higher $\Delta D/\Delta f$ value. This indicates that the energy dissipation of the adsorbed fibrinogen molecules along with the micro-vibration of the substrates is quite high. This phenomenon is only observed when adsorbed substances weakly interact with the surface; that is, fibrinogen molecules are adsorbed on the OMe-PRX-PMB surface in quite a soft manner. Why this kind of soft interaction only occurred on the OMe-PRX surface is still unclear. However, taking into account the dynamic nature of the OMe-PRX-PMB surface (Fig. 4 and 5), it is plausible that the dynamically movable nature of the OMe-PRX-PMB surface is responsible for the soft interaction with the fibrinogen molecules. Namely, the strong interaction with the surface was disturbed by dynamic mobility of the surface, thus, adsorbed fibrinogen molecules were continuously vibrating along with the micro-vibration of the surfaces to induce high-energy dissipation.

The conformational change of adsorbed fibrinogen on the dynamic polymer surfaces was estimated by means of the ELISA test using two types of primary antibodies, 49D2 and clone2 G2. H9, which can specifically bind to the N-terminus of the α-chain (1–16 peptide sequence) and the C-terminus of the γ-chain (434–453 peptide sequence) of the adsorbed fibrinogen, respectively. Fibrinogen molecules have two specific binding motifs responsible for cellular adhesion and aggregation. One is the dodecapeptide sequence existing close to the C-terminus of the γ-chain (400–411 peptide sequence), which is a binding site to GPIIb/IIIa on the platelet to finally trigger the activation of the platelet.[29] The other motif consists of the two RGD sequences in the α-chain (RGDF and RGDS on 95–98 and 572–575 peptide sequence), which is a binding site to the GPIIb/IIIa of the platelets as well as the $\alpha_v\beta_3$ integrin on various cells.[30] Previous ELISA studies on the adsorbed fibrinogen on polymer surfaces demonstrated that the surface presentation of the dodecapeptide sequence in adsorbed fibrinogen on material surfaces was well correlated with platelet adhesion whereas the relation of the presentation of the RGD motifs with the platelet adhesion was not so clear.[31,32] These results indicate that the C-terminus of the γ-chain, presenting the dodecapeptide sequence in the fibrinogen, is essential to induce the platelet-fibrinogen interaction, and the N-terminus of the α-chain itself does not seem to have a significant effect on the platelet adhesion. Therefore, it is considered that the exposure level of the C-terminus of the γ-chain is a good parameter to estimate the potency of the platelet adhesion. Therefore, how well the appearance of the platelet GPIIb/IIIa binding site in the C-terminus γ chain is suppressed could be a key to the development of ideal blood-contacting materials. Fig. 8 (a) shows the quantitative result of the secondary antibody binding specifically to the primary antibody

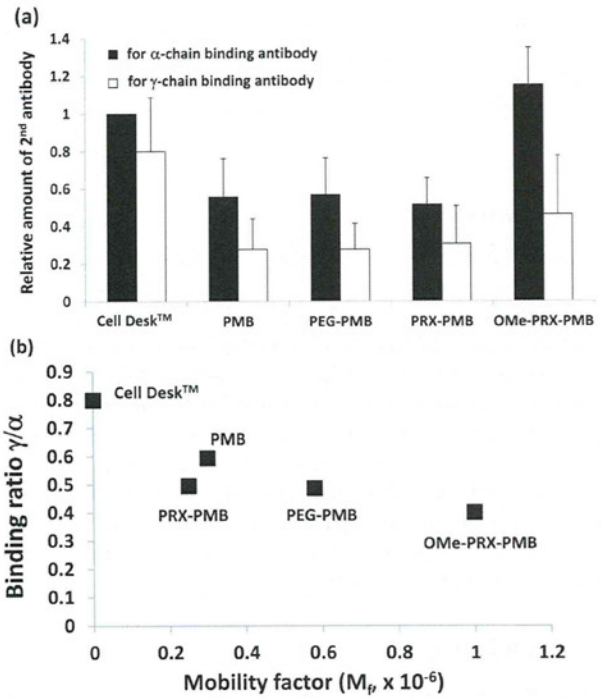


**Fig. 8** (a) Relative amount of secondary antibody to the specific binding primary antibody on N-terminus α- and C-terminus γ-chains of adsorbed fibrinogen estimated by ELISA assay (n = 6) and (b) plot of γ : α binding ratio *versus* $M_f$ values. Protein adsorption was carried out with 10% human plasma for 5 min contact prior to the ELISA test. The amount of secondary antibody was normalized to the amount of α-chain binding on the Cell Desk™.

bound to fibrinogen molecules. In the case of the Cell Desk™ surface, the amount of the binding antibody on both the γ- and α-chains was higher than that for other hydrophilic polymer surfaces, which indicates that the fibrinogen bound to the Cell Desk™ surface readily exposes both specific binding motifs. In contrast, other hydrophilic polymer surfaces showed a significantly lower level of the antibody binding in both the γ- and α-chains. This is possibly due to the quantitatively low level of adsorbed proteins as confirmed in the micro-BCA™ and QCM-D results. However, fibrinogen molecules on the OMe-PRX-PMB surface showed a quite interesting tendency. In spite of the significant amount of adsorbed plasma protein and fibrinogen, the amount of the secondary antibody for the C-terminus γ-chain binding antibody on the OMe-PRX-PMB surface was at a quite a low level compared to that on the Cell Desk™ surface (Figure S5†). This result suggests the possibility that inconsistent antibody binding was occurred due to the dynamic conformations which was induced by molecularly mobile segments in OMe-PRX-PMB. Fig. 8 (b) shows the plot of the antibody binding ratio (C-terminus γ-chain binding to N-terminus α-chain binding) *versus* the $M_f$ values. It is obvious that the C-terminus γ-chain binding ratio compared to that of the N-terminus α-chain, decreased as the $M_f$ value increased. Therefore, it is thought that the molecularly dynamic surfaces with high $\Delta D/\Delta f$ can induce moderate conformational changes no matter how many proteins are adsorbed on the surface.

### 3.4 Cellular responses to the PRX block copolymer surfaces

To estimate the effect of adsorbed plasma proteins on the biological responses, platelet and fibroblast adhesion tests were carried out by using the human PRP and NIH3T3 fibroblast. Fig. 9 (a) shows the result of platelet adhesion on the prepared polymer surfaces. Obviously, the Cell Desk™ surface induced large amounts of platelet adhesion on its surface, suggesting that the platelet adhesion is derived from a significant conformational change of the adsorbed proteins, including fibrinogen as confirmed by ELISA. In contrast, an insignificant number of adhering platelets was observed on all the prepared polymer surfaces. Fig. 9 (b) shows the quantitative result of adhering platelets along with the relative amount of the C-terminus γ-chain binding antibody. The resulting platelet adhesion was increased when the expression of the C-terminus γ-chain of the adsorbed fibrinogen was increased. This almost straightforward relationship is consistent with previously reported results.[31,32] The OMe-PRX-PMB surface showed a similar level of platelet adhesion in spite of the significant amount of adsorbed fibrinogen confirmed in the micro-BCA™ and QCM-D analyses. Several publications have stated that platelet adhesion normally increases in proportion to the amount of adsorbed fibrinogen.[33,34] However, the OMe-PRX-PMB surface showed a different tendency compared to those of the other materials surfaces. In particular, it is thought that the modulated conformational change of the adsorbed proteins, including fibrinogen on the dynamic OMe-PRX-PMB surface, can prevent platelet adhesion as discussed in Fig. 8 (b), in spite of the significant amounts of adsorbed proteins.

Fig. 10 (a) shows the resulting optical microscopic images of the polymer surfaces. Clearly, large numbers of fibroblasts were

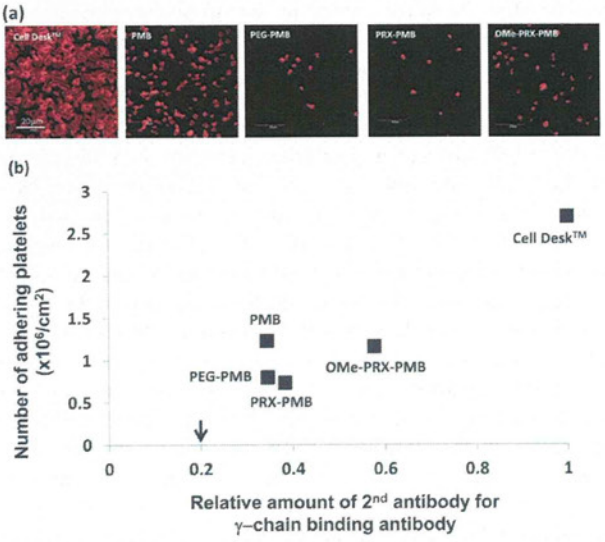


**Fig. 9** (a) Fluorescent microscopic image of adhering platelets and (b) quantitative analysis of adhering platelets using LDH assay (n = 3). The plot also shows the relative amount of the secondary antibody for the C-terminus γ-chain binding antibody (normalized to the Cell Desk™). The arrow indicates the background level of ELISA. PRP contact was carried out for 3 h at 37 °C. Scale bar = 200 μm.

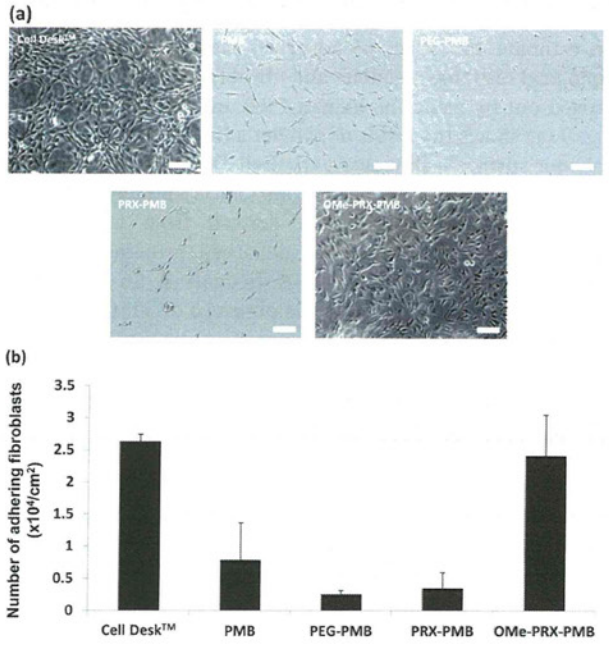


**Fig. 10** (a) Optical microscopic images of adhering NIH3T3 fibroblasts and (b) the number of adhering cells. The initial cell concentration was $1.1 \times 10^5$ mL$^{-1}$. Scale bar = 100 μm.

adhering and proliferating on the Cell Desk™ surface, which indicates that surface adsorbed proteins undergo significant conformational changes to induce both platelet and fibroblast adhesion. On the other hydrophilic polymer surfaces, almost no adhering fibroblasts were observed. Because the amount of adsorbed proteins was quite low on the series of hydrophilic surfaces, it could be said that the prepared hydrophilic control samples do not induce significant non-specific interaction with the protein molecules; thus, platelet and cell adhesion was prevented. In contrast, the OMe-PRX-PMB surface showed a significant number of adhering fibroblasts (Fig. 10 (b)). Although the adhering level was slightly lower than that of the Cell Desk™ surface, a significant amount of adhesive and proliferated fibroblasts were also observed on the OMe-PRX-PMB surface. Taking into account the result of low platelet adhesion on the OMe-PRX-PMB surface, this cellular response seems out of the ordinary. Normal cell adhesive surfaces induce strong platelet responses as well because on these surfaces, not only fibrinogen and the von Willebrand factor but also other cell adhesive proteins such as fibronectin and vitronectin showed significant conformational changes to present most of their specific binding motifs to integrins.[35–37] In the case of adsorbed fibrinogen on the OMe-PRX-PMB surface, the amount of the secondary antibody for the C-terminus γ-chain binding antibody, which indicates the presentation of a specific binding site for platelet GPIIb/IIIa, was eliminated at a much lower level than that for the Cell Desk™. This was so, even though the amount of adsorbed proteins was at a much higher level than that for the Cell Desk™. Analyzing the presentation of integrin binding motifs in various cell adhesive proteins on OMe-PRX-PMB is now been undertaken and the result will be discussed in our forthcoming paper. Although the investigation has not yet concluded, we speculate that modulated conformational change of the cell adhesive proteins in serum could be one of the significant reasons that the OMe-PRX-PMB surface showed enhanced fibroblast adhesion in spite of eliminating platelet adhesion.

## 4. Conclusions

Dynamic OMe-PRX-PMB surfaces prepared by molecularly movable block copolymer induced specific biological responses by modulating the conformation of adsorbed proteins, especially fibrinogen. This finding is presumably related to the highly responsive dynamic properties of the OMe-PRX-PMB surface, which are characterized by the anomalous results of the contact angle hysteresis, the molecular mobility factor was determined by QCM-D, fibrinogen adsorption, and its conformational analyses. These results suggest that in such a molecularly movable surface, flexibly responds to a dynamic biological environment, and could be a promising way to design new biomaterials for regulating biological responses.

## Acknowledgements

We thank Dr Tomo Ehashi and Dr Kwanwoo Nam for their helpful discussion on ELISA analysis, the cellular responses on the polymer surfaces, and AFM analysis.

## References

1 J. Brash, T. Horbett, *ACS symposium series*, 343, American Chemical Society, Washington, D.C., 1987.
2 T. Horbett, J. Brash, *ACS symposium series*, 602, American Chemical Society, Washington, D.C., 1995.
3 D. Absolom, W. Zingg and A. Neumann, *J. Biomed. Mater. Res.*, 1987, **21**, 161.
4 T. R. Kyriakides, K. J. Leach, A. S. Hoffman and B. D. Ratner, *Proc. Natl. Acad. Sci. U. S. A.*, 1999, **96**, 4449.
5 H. Chen, L. Yuan, W. Song, Z. Wu and D. Li, *Prog. Polym. Sci.*, 2008, **33**, 1059.
6 M. Yamato, Y. Akiyama, J. Kobayashi, J. Yang, A. Kikuchi and T. Okano, *Prog. Polym. Sci.*, 2007, **32**, 1123.
7 P. Roach, D. Farrar and C. C. Perry, *J. Am. Chem. Soc.*, 2005, **127**, 8168.
8 K. Rechendorff, M. B. Hovgaard, V. P. Zhdanov and F. Besenbacher, *Langmuir*, 2006, **22**, 10885.
9 M. A. Cole, N. H. Voelcker, H. Thissen and H. J. Griesser, *Biomaterials*, 2009, **30**, 1827.
10 E. A. Vogler, *Biomaterials*, 2012, **33**, 1201.
11 T. Ooya, M. Eguchi and N. Yui, *J. Am. Chem. Soc.*, 2003, **125**, 13016.
12 N. Yui and T. Ooya, *Chem.–Eur. J.*, 2006, **12**, 6730.
13 H. Utsunomiya, R. Katoono, N. Yui, T. Sugiura, Y. Kubo, Y. Kato and A. Tsuji, *Macromol. Biosci.*, 2008, **8**, 655.
14 H. Hyun and N. Yui, *Macromol. Rapid Commun.*, 2011, **32**, 326.
15 H. Hyun and N. Yui, *Macromol. Biosci.*, 2011, **11**, 765.
16 T. Ooya, H. S. Choi, A. Yamashita, N. Yui, Y. Sugaya, A. Kano, A. Maruyama, H. Akita, K. Kogure and H. Harashima, *J. Am. Chem. Soc.*, 2006, **28**, 3852.
17 A. Yamashita, N. Yui, T. Ooya, A. Kano, A. Maruyama, H. Akita, K. Kogure and H. Harashima, *Nat. Protoc.*, 2006, **1**, 2861.
18 A. Yamashita, D. Kanda, R. Katoono, N. Yui, T. Ooya, A. Maruyama, H. Akita and H. Harashima, *J. Controlled Release*, 2008, **131**, 137.
19 Y. Yamada, T. Nomura, H. Harashima, A. Yamashita, R. Katoono and N. Yui, *Biol. Pharm. Bull.*, 2010, **33**, 1218.
20 Y. Yamada, M. Hashida, T. Nomura, H. Harashima, Y. Yamasaki, K. Kataoka, A. Yamashita, R. Katoono and N. Yui, *ChemPhysChem*, 2012, **13**, 1161.

21 Y. Yamada, T. Nomura, H. Harashima, A. Yamashita and N. Yui, *Biomaterials*, 2012, **33**, 3952.
22 Y. Inoue, L. Ye, K. Ishihara and N. Yui, *Colloids Surf., B*, 2012, **89**, 223.
23 Y. Mitsukami, M. S. Donovan, A. B. Lowe and C. L. McCormick, *Macromolecules*, 2001, **34**, 2248.
24 S. Zalipsky, C. Gilon and A. Zilkha, *Eur. Polym. J.*, 1983, **19**, 1177.
25 A. G. Hemmersam, K. Rechendorff, F. Besenbacher, B. Kasemo and D. S. Sutherland, *J. Phys. Chem. C*, 2008, **112**, 4180.
26 Y. Hong, S. H. Ye, A. Nieponice, L. Soletti, D. A. Vorp and W. R. Wagner, *Biomaterials*, 2009, **30**, 2457.
27 K. Ishihara, T. Ueda and N. Nakabayashi, *Polym. J.*, 1990, **22**, 355.
28 K. Futamura, R. Matsuno, T. Konno, M. Takai and K. Ishihara, *Langmuir*, 2008, **24**, 10340.
29 M. B. Gorbet and M. V. Sefton, *Biomaterials*, 2004, **25**, 5681.
30 J. M. Grunkemeier, W. B. Tsai, C. D. McFarland and T. A. Horbet, *Biomaterials*, 2000, **21**, 2243.
31 Y. Wu, F. I. Simonovsky, B. D. Ratner and T. A. Horbett, *J. Biomed. Mater. Res., Part A*, 2005, **74A**, 722.
32 W. B. Tsai, J. M. Grunkemeier and T. A. Horbett, *J. Biomed. Mater. Res.*, 2003, **67A**, 1255.
33 T. H. Fischer, H. S. Thatte, T. C. Nichols, D. E. Bender-Neal, D. A. Bellinger and J. N. Vournakis, *Biomaterials*, 2005, **26**, 5433.
34 B. Sivaraman and R. A. Latour, *Biomaterials*, 2010, **31**, 832.
35 A. M. Moulin, S. J. O'Shea, R. A. Badley, P. Doyle and M. E. Welland, *Langmuir*, 1999, **15**, 8776.
36 A. J. Garcia, M. D. Vega and D. Boettinger, *Mol. Biol. Cell.*, 1999, **10**, 785.
37 B. G. Keselowsky, D. M. Collard and A. J. Garcia, *J. Biomed. Mater. Res.*, 2003, **66A**, 247.

JOURNAL OF THE MECHANICAL BEHAVIOR OF BIOMEDICAL MATERIALS ▮ (▮▮▮▮) ▮▮▮–▮▮▮

Available online at www.sciencedirect.com

SciVerse ScienceDirect

www.elsevier.com/locate/jmbbm

Research Paper

# Grafting of poly(2-methacryloyloxyethyl phosphorylcholine) on polyethylene liner in artificial hip joints reduces production of wear particles

Toru Moro[a,b,*], Masayuki Kyomoto[a,c,d], Kazuhiko Ishihara[c], Kenichi Saiga[a,c,d], Masami Hashimoto[e], Sakae Tanaka[b], Hideya Ito[b], Takeyuki Tanaka[b], Hirofumi Oshima[b], Hiroshi Kawaguchi[b], Yoshio Takatori[a,b]

[a]Division of Science for Joint Reconstruction, Graduate School of Medicine, The University of Tokyo, 7-3-1 Hongo, Bunkyo-ku, Tokyo 113-8655, Japan
[b]Sensory & Motor System Medicine, Faculty of Medicine, The University of Tokyo, 7-3-1 Hongo, Bunkyo-ku, Tokyo 113-8655, Japan
[c]Department of Materials Engineering, School of Engineering, The University of Tokyo, 7-3-1 Hongo, Bunkyo-ku, Tokyo 113-8655, Japan
[d]Research Department, KYOCERA Medical Corporation, 3-3-31 Miyahara, Yodogawa-ku, Osaka 532-0003, Japan
[e]Materials Research and Development Laboratory, Japan Fine Ceramics Center, 2-4-1 Mutsuno, Atsuta-ku, Nagoya 456-8587, Japan

ARTICLE INFO

*Article history:*
Received 20 April 2012
Received in revised form
7 March 2013
Accepted 18 March 2013

*Keywords:*
Artificial hip joint
Total hip arthroplasty
Periprosthetic osteolysis
Aseptic loosening
Polyethylene
Surface modification

ABSTRACT

Despite improvements in the techniques, materials, and fixation of total hip arthroplasty, periprosthetic osteolysis, a complication that arises from this clinical procedure and causes aseptic loosening, is considered to be a major clinical problem associated with total hip arthroplasty. With the objective of reducing the production of wear particles and eliminating periprosthetic osteolysis, we prepared a novel hip polyethylene (PE) liner whose surface graft was made of a biocompatible phospholipid polymer—poly(2-methacryloyloxyethyl phosphorylcholine (MPC)). This study investigated the wear resistance of the poly(MPC)-grafted cross-linked PE (CLPE; MPC-CLPE) liner during $15 \times 10^6$ cycles of loading in a hip joint simulator. The gravimetric analysis showed that the wear of the acetabular liner was dramatically suppressed in the MPC-CLPE liner, as compared to that in the non-treated CLPE liner. Analyses of the MPC-CLPE liner surface revealed that it suffered from no or very little wear even after the simulator test, whereas the CLPE liners suffered from substantial wears. The scanning electron microscope (SEM) analysis of the wear particles isolated from the lubricants showed that poly(MPC) grafting dramatically decreased the total number, area, and volume of the wear particles. However, there was no significant difference in the particle size distributions, and, in particular, from the SEM image, it was observed that particles with diameters less than 0.50 μm were present in the range of the highest frequency. In addition, there were no significant differences in the particle size descriptors and particle shape descriptors.

*Corresponding author at: Division of Science for Joint Reconstruction, Graduate School of Medicine, The University of Tokyo, 7-3-1 Hongo, Bunkyo-ku, Tokyo 113-8655, Japan. Tel.: +81 3 3815 5411x30474; fax: +81 3 3818 4082.
*E-mail address:* moro-ort@h.u-tokyo.ac.jp (T. Moro).

1751-6161/$ - see front matter 
http://dx.doi.org/10.1016/j.jmbbm.2013.03.011

The results obtained in this study show that poly(MPC) grafting markedly reduces the production of wear particles from CLPE liners, without affecting the size of the particles. These results suggest that poly(MPC) grafting is a promising technique for increasing the longevity of artificial hip joints.



## 1. Introduction

Sir John Charnley introduced the use of polyethylene (PE) components in total hip arthroplasty (THA) in the 1960s, and since then, these components have been extensively used for 50 years (Charnley, 1961). However, aseptic loosening resulting from periprosthetic osteolysis—which is a clinical complication arising from THA—is the prevalent cause of revision surgery (Bozic et al., 2009). Previous studies have revealed that PE particles generated from liners play a major etiological role in periprosthetic osteolysis. Macrophage phagocytosis of the PE particles is followed by the secretion of prostaglandin E2 (PGE2) and cytokines, which induce the receptor activator of the NF-κB ligand (RANKL) expression, consequently resulting in osteoclastogenesis and bone resorption (Harris, 2004; Jacobs et al., 2001). Further, periprosthetic osteolysis is closely related to the rate of PE wear and the characteristics of the wear particles (Catelas and Jacobs, 2010). Hence, various attempts have been made to improve the wear resistance of PE liners, such as enhancing the cross-linking of PE (CLPE) (Callaghan et al., 2008).

In the previous studies, we introduced a nanometer-scaled poly(2-methacryloyloxyethyl phosphorylcholine (MPC)) grafting layer on the surface of CLPE liners. We found that such type of grafting dramatically decreased the wear of the liner surface (Moro et al., 2009, 2006). In the present study, we investigated the effect of poly(MPC) grafting on the production of wear particles, using a hip wear simulator up to $15 \times 10^6$ cycles.

## 2. Materials and methods

### 2.1. Poly(MPC) grafting

Nanometer-scaled grafting (100–150 nm in thickness) of the poly (MPC) onto the PE liner surface was carried out by a photo-induced polymerization technique. The CLPE liners (K-MAX® CLQC; KYOCERA Medical Corp., Osaka, Japan) were immersed in an acetone solution containing 10 mg/mL of benzophenone for 30 s and then dried at room temperature to remove the acetone. Then, MPC (NOF Corp., Tokyo, Japan) (Ishihara et al., 1990) was dissolved in degassed pure water to obtain a 0.50 mol/L MPC aqueous solution, and the benzophenone-coated CLPE liners were immersed in this solution. Photoinduced graft polymerization was carried out on the CLPE liner surface using ultraviolet irradiation (UVL-400HA ultra-high-pressure mercury lamp; Riko-Kagaku Sangyo Co., Ltd., Funabashi, Japan) with an intensity of 5.0 mW/cm$^2$ at 60 °C for 90 min; subsequently, a filter (Model D-35; Toshiba Corp., Tokyo, Japan) was used to restrict the passage of ultraviolet light to wavelengths of 350±50 nm. After the poly (MPC)-grafted CLPE (MPC-CLPE) liners were polymerized, they were washed with pure water and ethanol and dried at room temperature. These specimens were then sterilized by 25-kGy gamma rays under $N_2$ gas (Kyomoto et al., 2008).

### 2.2. Hip joint simulator

A 12-station hip simulator (MTS Systems Corp., Eden Prairie, MN) with CLPE and MPC-CLPE liners, each with inner and outer diameters of 26 and 52 mm, respectively, was used for the hip simulator wear test performed according to the ISO Standard 14242-3. A Co–Cr alloy femoral head with a diameter of 26 mm (K-MAX® HH-02; KYOCERA Medical Corp.) was used as the femoral component. A biaxial rocking motion was applied to the head/cup interface via an offset bearing assembly with an inclined angle of +23°. Both the loading and motion were synchronized at 1 Hz. According to the double-peaked Paul-type physiologic hip load, the applied peak loads were 1793 and 2744 N (Paul, 1967). Bovine calf serum (25 vol%) diluted in distilled water was used as a lubricant. Sodium azide (10 mg/L) and EDTA (20 mM) were added to prevent microbial contamination and to minimize the formation of calcium phosphate on the implant surface.

The simulator was run up to $15 \times 10^6$ cycles. The liners were cleaned and weighed on a microbalance (Sartorius Genius ME215S, Sartorius AG, Goettingen, Germany) at intervals of $0.5 \times 10^6$ cycles. The lubricant was collected and stored at −20 °C for further analysis. Wear was determined from the weight loss of each liner and corrected by cyclically loaded soak controls according to the ISO Standard 14242-2. The wear rates were determined by linear regression.

After complete loading, morphological changes in the liner surface were measured using a three-dimensional (3D) coordinate measuring machine (BHN-305, Mitsutoyo Corp., Kawasaki, Japan) and reconstructed using 3D modeling software (Imageware, Siemens PLM Software Inc., TX, USA). The liner surface was analyzed using a confocal scanning laser microscope (OLS1200, Olympus, Tokyo, Japan), as previously reported.

The wear particles were isolated from the bovine serum solution. For isolating the wear particles from the lubricant, the lubricant was incubated with 5.0 mol/L of NaOH solution for 3 h at 65 °C after it was tested, in order to digest adhesive proteins that were degraded and precipitated. To avoid artifacts, contaminating proteins were removed by extraction with sugar solution (1.20 g/cm$^3$ and 1.05 g/cm$^3$) and isopropyl alcohol solutions (0.98 and 0.90 g/cm$^3$). After the lubricant was centrifuged at 25,500 rpm for 3 h at 5 °C, the particles were collected, subjected to sequential filtrations (minimum pore size of 0.1 μm) (Fisher et al., 2004; Tipper et al., 2006), and subsequently dried. The filter was then sputter coated with gold palladium and digitally imaged on a field emission scanning electron microscope (JSM-6330F, JEOL Datum Co., Ltd, Tokyo, Japan). An image-processing program (Scion image, Scion Corp., Frederick, MD) based on the

Please cite this article as: Moro, T., et al., Grafting of poly(2-methacryloyloxyethyl phosphorylcholine) on polyethylene liner in artificial hip joints reduces production of wear particles. Journal of the Mechanical Behavior of Biomedical Materials (2013), http://dx.doi.org/10.1016/j.jmbbm.2013.03.011

NIH image software was used to measure the total number, area, and volume of the wear particles per $10^6$ cycles (Campbell et al., 1996; Dean et al., 1999). Two size descriptors, namely, the equivalent circle diameter (ECD) and the diameter (D), and two shape descriptors, namely, the aspect ratio (AR) and roundness (R), were used to define each wear particle, according to ASTM F1877-98. Each parameter is defined as follows. ECD is defined as the diameter of a circle with an area that is equivalent to that of one wear particle. Diameter is defined using the maximum dimensions determined by the SEM analysis. Aspect ratio is defined as the ratio of the major diameter to the minor diameter. It should be noted that the major diameter is the longest straight line that can be drawn between any two points on the outline. On the other hand, the minor diameter is the longest line that is perpendicular to the major diameter. Roundness is a measure of how closely a wear particle resembles a circle; its values range from 0 to 1, with a perfect circle having a roundness value of 1.

### 2.3. *Statistical analysis*

The significance of differences was determined by the student's *t*-test. All statistical analyses were performed using add-in software (Statcel 2; OMS publishing Inc, Tokorozawa, Japan) on a computerized worksheet (Microsoft Excel® 2003; Microsoft Corp, Redmond, WA).

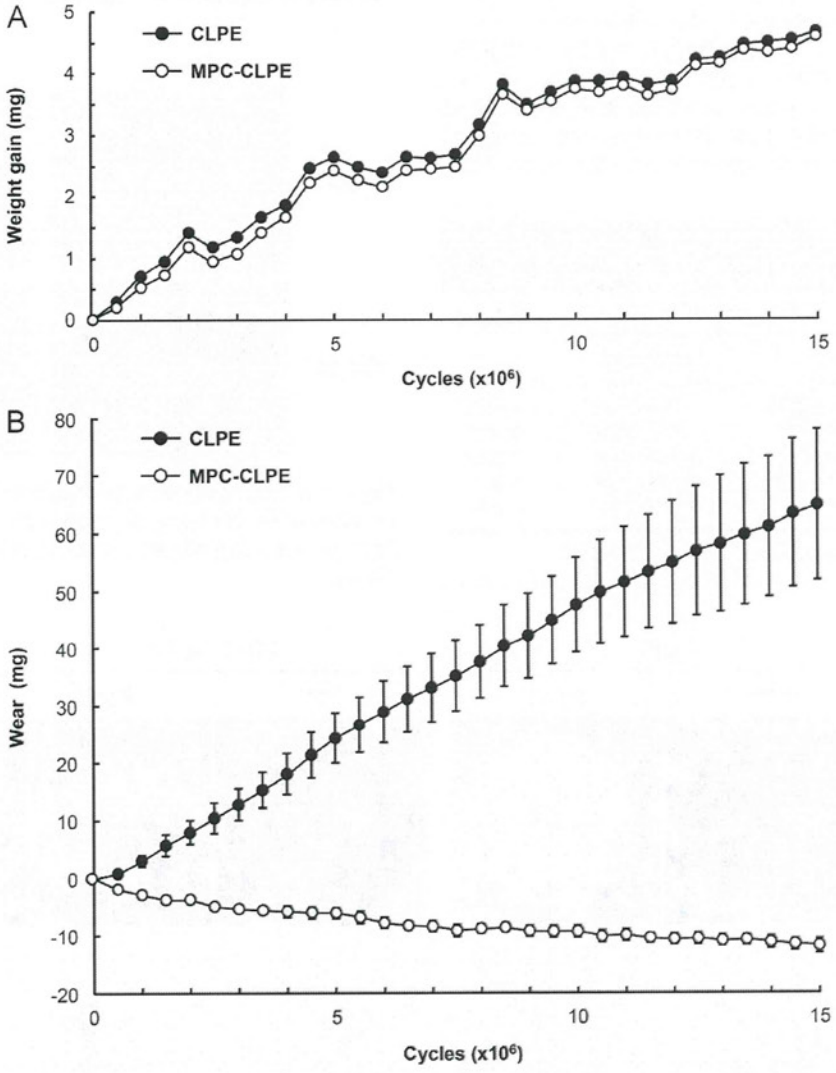


**Fig. 1 – Wear amounts of cross-linked PE liners with or without MPC grafting in the THA simulator. (A) Load-soak controls. Fluid absorption of the liners that were axially loaded cyclically to the acetabular liners with the same pressure as the THA simulator, but without rotational motion. Data are expressed as means (symbols) for 2 inserts/group. (B) Time course of wear amount in the THA simulator during $15 \times 10^6$ cycles of rotational motion and axial loading against Co–Cr alloy femoral heads. The wear amount was estimated from the weight loss of the inserts after correction by the average weight gain in the respective load-soak controls (weight loss in the THA simulator+average of weight gain in the load-soak control). Data are expressed as means (symbols)±standard deviation (SD) for 4 liners/group.**

Please cite this article as: Moro, T., et al., Grafting of poly(2-methacryloyloxyethyl phosphorylcholine) on polyethylene liner in artificial hip joints reduces production of wear particles. Journal of the Mechanical Behavior of Biomedical Materials (2013), http://dx.doi.org/10.1016/j.jmbbm.2013.03.011

## 3. Results

Two types of load-soak control liners, which were only loaded axially to the femoral heads and without any rotational motion in the simulator, showed comparable weight gains during the $15 \times 10^6$ cycles, irrespective of whether poly(MPC) grafting (Fig. 1A) was carried out; this observation confirmed that weight gain was caused by the absorption of the fluid by the liner material, and not by the fluid that was retained in the surface poly(MPC) layer (Kyomoto et al., 2011; Moro et al., 2006, 2009). We then evaluated gravimetric wear by assessing the weight loss of the liners after correction by the average weight gain in the respective load-soak controls. The gravimetric analysis performed in the hip simulator study showed that the CLPE liners suffered from a total weight loss of $64.8 \pm 11.7$ mg (mean ± standard deviation) after $15 \times 10^6$ cycles of loading (Fig. 1B). In contrast, it was found that the MPC-CLPE liners continued to gain weight, showing a total weight gain of $13.1 \pm 1.2$ mg. This weight gain might be at least partially attributed to greater fluid (e.g., water, proteins, and lipids) absorption in the tested liners than in the load-soak controls, suggesting the underestimation of the load-soak control, as reported previously (Dumbleton et al., 2006; Muratoglu et al., 2001; Oral et al., 2006; Shen et al., 2011). When the wear rate was counted at an interval of every $10^6$ cycles, poly(MPC) grafting was shown to maintain similar wear resistance in 0–1 ($p=0.0016$), 4–5 ($p=0.0019$), 9–10 ($p=0.0022$), 14–15 ($p=0.0075$), and the total ($p=0.002$) intervals (Table 1).

3D coordinate measurements of the MPC-CLPE liner surface revealed no or very little detectable volumetric wear, while the cross-linked PE liners suffered from substantial wears (Fig. 2A). The confocal scanning laser microscopic analysis of the liner surface showed that the original machine marks that are clearly visible before the loading still remained on the MPC-CLPE liner surface, although they were completely obliterated on the cross-linked PE liner.

**Table 1 – Wear rate estimated by the corrected weight loss of CLPE and MPC-CLPE liners.**

| Test period ($10^6$ cycles) | Wear rate (mg/$10^6$ cycles) | | $p$-value |
|---|---|---|---|
| | CLPE | MPC-CLPE | |
| 0–1 | 2.34± 0.99 | −3.43±0.42 | 0.0016 |
| 4–5 | 5.47±1.09 | −1.05±0.06 | 0.0019 |
| 9–10 | 4.85±0.91 | −0.47±0.08 | 0.0022 |
| 14–15 | 3.60±1.22 | −0.73±0.23 | 0.0075 |
| Total | 4.01±0.87 | −1.09±0.08 | 0.0020 |

Data are expressed as mean ± standard deviation (SD).

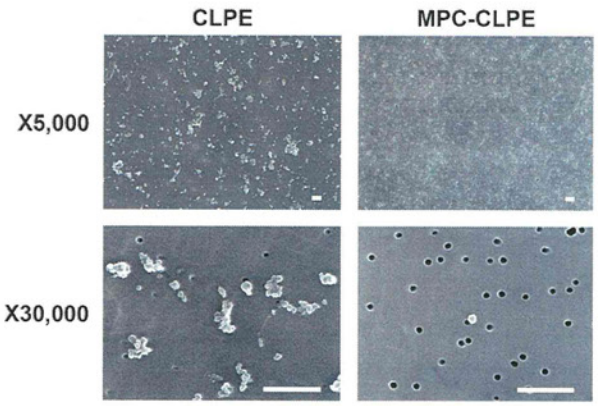


**Fig. 3 – Scanning electron microscopic images of the wear particles from CLPE and MPC-CLPE liners. Low (top) and high (bottom) magnifications of the SEM images. Scale bars: 1.0 μm.**

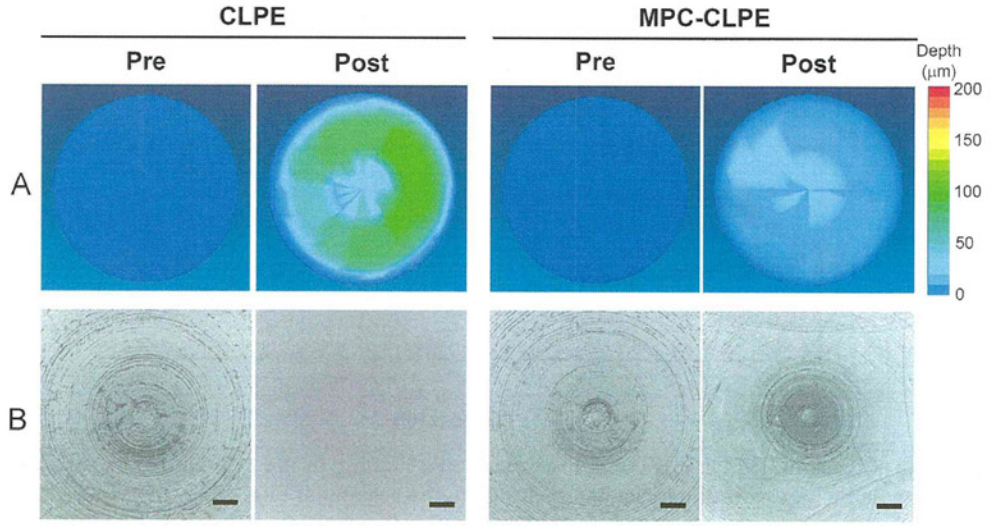


**Fig. 2 – Optical findings of the surfaces of the two liners in the THA simulator. (A) Three-dimensional morphometric analyses of surfaces of the CLPE and MPC-CLPE liners before (pre) and after (post) $15 \times 10^6$ cycles. (B) Confocal scanning laser microscopic analysis of the contact areas in the two liner surfaces before (pre) and after (post) $15 \times 10^6$ cycles. Scale bars: 200 μm.**

Please cite this article as: Moro, T., et al., Grafting of poly(2-methacryloyloxyethyl phosphorylcholine) on polyethylene liner in artificial hip joints reduces production of wear particles. Journal of the Mechanical Behavior of Biomedical Materials (2013), http://dx.doi.org/10.1016/j.jmbbm.2013.03.011

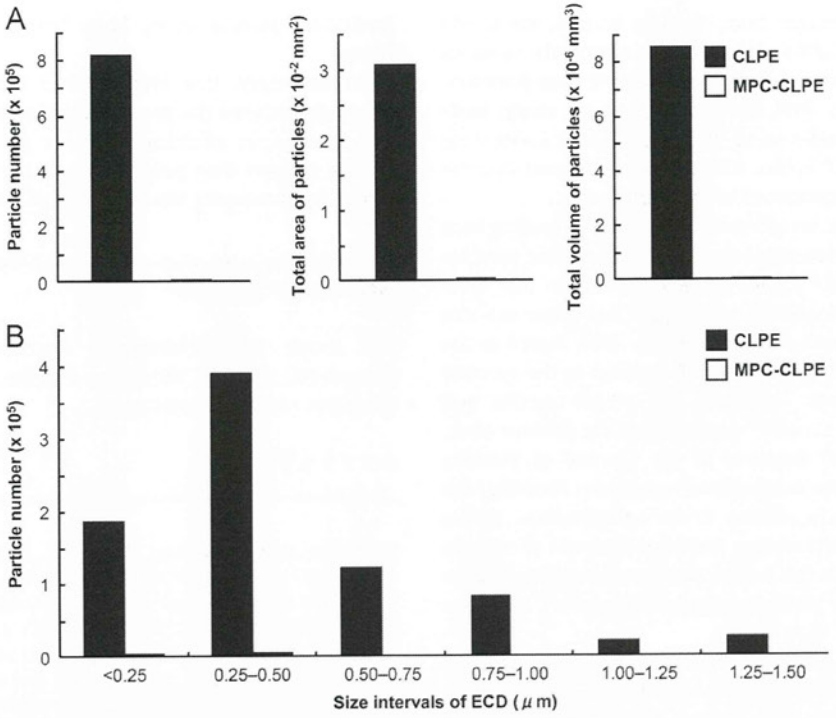


**Fig. 4 – Analyses of wear particles isolated from lubricants in the hip simulator. (A) The graphs show the total number, area, and volume of the wear particles per $10^6$ cycles. (B) Number of particles per $10^6$ cycles in each size range of the equivalent circle diameter from CLPE and MPC-CLPE liners.**

**Table 2 – Assessments of the particle from CLPE and MPC-CLPE liners using size and shape descriptors.**

| Particle characterization | CLPE | MPC-CLPE | *p*-value |
|---|---|---|---|
| ECD (μm) | 0.18±0.13 | 0.13±0.06 | 0.0000 |
| Diameter (μm) | 0.28±0.24 | 0.19±0.11 | 0.0001 |
| Aspect ratio | 2.31±0.79 | 2.10±0.51 | 0.0211 |
| Roundness | 0.83±0.22 | 0.92±0.13 | 0.0000 |

Two size descriptors, i.e., equivalent circle diameter (ECD) and diameter (*D*), and two shape descriptors, i.e., aspect ratio (AR) and roundness (R), were used to define each particle. Data are expressed as mean±standard deviation (SD).

The SEM analysis of the wear particles isolated from the lubricants indicated that poly(MPC) grafting dramatically decreased the total number, area, and volume of the wear particles by 99.3%, 99.9% and 99.9%, respectively (Fig. 3, Fig. 4A). However, there was no significant difference in the particle size distributions expressed by the equivalent circle diameter of each liner, and, in particular, from the SEM image, it was observed that particles with diameters less than 0.50 μm were present in the range of the highest frequency (Fig. 4C). In addition, there were no significant differences in the particle size descriptors, equivalent circle diameter ($p<0.0001$), and diameter ($p=0.0001$), as well as in the particle shape descriptors, aspect ratio ($p=0.0211$), and roundness ($p<0.0001$) (Table 2).

## 4. Discussion

An MPC molecule is one of the synthesized phospholipids and mimicks the surface of cellmembranes (Ishihara et al., 1990). Thus, poly(MPC) grafting onto medical devices makes their surface hydrophilic and biocompatible. Further, a thin film of water is formed under physiological conditions (Kitano et al., 2003). At the time of writing, the MPC polymers are applied to the surface of intravascular stents (Kuiper and Nordrehaug, 2000; Palmer et al., 2004), soft contact lenses (Selan et al., 2009), and artificial lungs and hearts (Kihara et al., 2003; Snyder et al., 2007) under the authorization of the U. S. Food and Drug Administration (FDA).

Because the PE liners are subjected to multidirectional heavy loads, we used a photoinduced radical graft polymerization technique for grafting. This technique produces a strong C–C covalent bond between a carbon atom of PE and the end-group of a poly(MPC) main chain. The advantages of this technique are that it not only results in the production of a uniform poly(MPC) layer (100–150 nm in thickness) but also causes a negligible effect on the physical and mechanical properties of the CLPE substrate (Ishihara et al., 2000; Kyomoto et al., 2007). Using this technique, we produced a new MPC-CLPE acetabular liner (Aquala® liner; KYOCERA Medical Corp.,) and the Japanese government (Ministry of Health, Labor, and Welfare) approved its clinical use in artificial hip joints in April 2011.

In addition to wear resistance, the durability of the nanometer-scaled poly(MPC) layer is also of major concern.

Please cite this article as: Moro, T., et al., Grafting of poly(2-methacryloyloxyethyl phosphorylcholine) on polyethylene liner in artificial hip joints reduces production of wear particles. Journal of the Mechanical Behavior of Biomedical Materials (2013), http://dx.doi.org/10.1016/j.jmbbm.2013.03.011

When this layer is removed from the liner surface, the steady wear rate of the MPC-CLPE liner increases to almost the same (or slight lower) level as that of the untreated CLPE liner (Kyomoto et al., 2011; Moro et al., 2006, 2010). In the present study, MPC-CLPE liners showed weight gains and a significantly lower wear rate during the $15 \times 10^6$ cycles. This finding confirmed that the poly(MPC) layer was maintained even after the test.

In the present study, we showed that poly(MPC) grafting onto the CLPE liner surface decreased the production of wear particles by 99% during $15 \times 10^6$ cycles of loading in the hip wear simulator. Moreover, poly(MPC) grafting did not affect the size of the wear particles and their distribution. With regard to the relationship between the number of PE particles in the synovial tissue and periprosthetic osteolysis, the critical number was reported to be around $1.0 \times 10^{10}$ particles/g tissue (Kadoya et al., 1998). Thus, a marked decrease in the number of particles presumably reduces the incidence of osteolysis. Recently, the size of wear products in relation to the complications arising from metal-on-metal articulation has been the topic of concern (Hosman et al., 2010). In this regard, our results suggest that the influences of the wear products of poly(MPC)-grafted liners are similar to those of the CLPE liners.

There are three limitations of this study, with the first being underestimation in the load-soak test (ISO 14242-2) for determining the cause of weight gain in the liner. When using the gravimetric method, the weight loss in the tested liners is corrected for by subtracting the weight gain in the load-soak controls; however, this correction cannot be precisely achieved because only the tested liners are continuously subjected to load and motion. Fluid absorption in the tested liners is generally slightly higher than that in the load-soak controls. Consequently, the correction for fluid absorption through the use of the load-soak control as the correction factor leads to a slight underestimation of the actual weight loss. This underestimation has previously been reported, particularly in several reports on wear-resistant articulating surfaces (Dumbleton et al., 2006; Muratoglu et al., 2001; Oral et al., 2006; Shen et al., 2011). Because of this underestimation, wear could not be quantified by gravimetric analysis; however, weight change in the MPC-CLPE liners suggests the considerable wear-resistance of them. In the present study, we also analyzed the surface of the liner and the amount of wear particles generated from the liner, as well as confirmed that wear resistance of the acetabular liners was considerably improved by poly(MPC) grafting.

The second limitation of this study is the difference between the in vitro study and clinical settings. This difference was a matter of concern in the case of Hylamer (Graeter and Nevins, 1998; Huddleston et al., 2010). We do, however, believe that this issue is relatively insignificant as compared to that with regard to other materials, because poly(MPC)-grafted particles are biologically inert and do not cause the subsequent bone resorptive responses (Moro et al., 2004). Moreover, to the best of our knowledge, there are no reports on the complications of medical devices using MPC polymers.

The third limitation is that we used only Co–Cr alloy heads with a diameter of 26 mm. In clinical settings, there seems to be a tendency to choose large heads and thin acetabular liners in order to reduce the incidence of dislocation. We believe that this drawback is partially offset by the long duration of simulation. At present, we are conducting additional studies using large heads and thin acetabular liners.

In summary, this study shows that poly(MPC) grafting markedly reduces the production of wear particles from CLPE liners, without affecting the size of the particles. These results suggest that poly(MPC) grafting is a promising technique for increasing the longevity of artificial hip joints.

## Acknowledgments

We thank Kozo Nakamura, Tomohiro Konno, Noboru Yamawaki, Fumiaki Miyaji, and Reiko Yamaguchi for their excellent technical assistance.

## REFERENCES

Bozic, K.J., Kurtz, S.M., Lau, E., Ong, K., Vail, T.P., Berry, D.J., 2009. The epidemiology of revision total hip arthroplasty in the United States. Journal of Bone & Joint Surgery 91, 128–133.

Callaghan, J.J., Cuckler, J.M., Huddleston, J.I., Galante, J.O., 2008. How have alternative bearings (such as metal-on-metal, highly cross-linked polyethylene, and ceramic-on-ceramic) affected the prevention and treatment of osteolysis? Journal of the American Academy of Orthopaedic Surgeons 16 (Suppl. 1), S33–38.

Campbell, P., Doorn, P., Dorey, F., Amstutz, H.C., 1996. Wear and morphology of ultra-high molecular weight polyethylene wear particles from total hip replacements. Proceedings of the Institution of Mechanical Engineers Part H 210, 167–174.

Catelas, I., Jacobs, J.J., 2010. Biologic activity of wear particles. Instructional Course Lectures 59, 3–16.

Charnley, J., 1961. Arthroplasty of the hip. A new operation. Lancet 1, 1129–1132.

Dean, D.D., Schwartz, Z., Liu, Y., Blanchard, C.R., Agrawal, C.M., Mabrey, J.D., Sylvia, V.L., Lohmann, C.H., Boyan, B.D., 1999. The effect of ultra-high molecular weight polyethylene wear debris on MG63 osteosarcoma cells in vitro. Journal of Bone and Joint Surgery—American Volume 81, 452–461.

Dumbleton, J.H., D'Antonio, J.A., Manley, M.T., Capello, W.N., Wang, A., 2006. The basis for a second-generation highly cross-linked UHMWPE. Clinical Orthopaedics and Related Research 453, 265–271.

Fisher, J., McEwen, H.M., Tipper, J.L., Galvin, A.L., Ingram, J., Kamali, A., Stone, M.H., Ingham, E., 2004. Wear, debris, and biologic activity of cross-linked polyethylene in the knee: benefits and potential concerns. Clinical Orthopaedics and Related Research 428, 114–119.

Graeter, J.H., Nevins, R., 1998. Early osteolysis with Hylamer acetabular liners. Journal of Arthroplasty 13, 464–466.

Harris, W.H., 2004. Conquest of a worldwide human disease: particle-induced periprosthetic osteolysis. Clinical Orthopaedics and Related Research 429, 39–42.

Hosman, A.H., van der Mei, H.C., Bulstra, S.K., Busscher, H.J., Neut, D., 2010. Effects of metal-on-metal wear on the host immune system and infection in hip arthroplasty. Acta Orthopaedica 81, 526–534.

Huddleston, J.I., Harris, A.H., Atienza, C.A., Woolson, S.T., 2010. Hylamer vs conventional polyethylene in primary total hip arthroplasty: a long-term case-control study of wear rates and osteolysis. Journal of Arthroplasty 25, 203–207.

Ishihara, K., Iwasaki, Y., Ebihara, S., Shindo, Y., Nakabayashi, N., 2000. Photoinduced graft polymerization of 2-methacryloyloxyethyl phosphorylcholine on polyethylene membrane surface for obtaining blood cell adhesion resistance. Colloids and Surfaces B: Biointerfaces 18, 325–335.

Please cite this article as: Moro, T., et al., Grafting of poly(2-methacryloyloxyethyl phosphorylcholine) on polyethylene liner in artificial hip joints reduces production of wear particles. Journal of the Mechanical Behavior of Biomedical Materials (2013), http://dx.doi.org/10.1016/j.jmbbm.2013.03.011

Ishihara, K., Ueda, T., Nakabayashi, N., 1990. Preparation of phospholipid polymers and their properties as polymer hydrogel membrane. Polymer Journal 22, 355–360.

Jacobs, J.J., Roebuck, K.A., Archibeck, M., Hallab, N.J., Glant, T.T., 2001. Osteolysis: basic science. Clinical Orthopaedics and Related Research 393, 71–77.

Kadoya, Y., Kobayashi, A., Ohashi, H., 1998. Wear and osteolysis in total joint replacements. Acta Orthopaedica Scandinavica 278, 1–16.

Kihara, S., Yamazaki, K., Litwak, K., Litwak, P., Kameneva, M., Ushiyama, H., Tokuno, T., Borzelleca, D., Umezu, M., Tomioka, J., Tagusari, O., Akimoto, T., Koyanagi, H., Kurosawa, H., Kormos, R., Griffith, B., 2003. In vivo evaluation of a MPC polymer coated continuous flow left ventricular assist system. Artificial Organs 27, 188–192.

Kitano, H., Imai, M., Mori, T., Gemmei-Ide, M., Yokoyama, Y., Ishihara, K., 2003. Structure of water in the vicinity of phospholipid analogue copolymers as studied by vibrational spectroscopy. Langmuir 19, 10260–10266.

Kuiper, K.K., Nordrehaug, J.E., 2000. Early mobilization after protamine reversal of heparin following implantation of phosphorylcholine-coated stents in totally occluded coronary arteries. American Journal of Cardiology 85, 698–702.

Kyomoto, M., Moro, T., Konno, T., Takadama, H., Kawaguchi, H., Takatori, Y., Nakamura, K., Yamawaki, N., Ishihara, K., 2007. Effects of photo-induced graft polymerization of 2-methacryloyloxyethyl phosphorylcholine on physical properties of cross-linked polyethylene in artificial hip joints. Journal of Materials Science: Materials in Medicine 18, 1809–1815.

Kyomoto, M., Moro, T., Miyaji, F., Konno, T., Hashimoto, M., Kawaguchi, H., Takatori, Y., Nakamura, K., Ishihara, K., 2008. Enhanced wear resistance of orthopaedic bearing due to the cross-linking of poly(MPC) graft chains induced by gamma-ray irradiation. Journal of Biomedical Materials Research Part B: Applied Biomaterials 84, 320–327.

Kyomoto, M., Moro, T., Takatori, Y., Kawaguchi, H., Ishihara, K., 2011. Cartilage-mimicking, high-density brush structure improves wear resistance of crosslinked polyethylene: a pilot study. Clinical Orthopaedics and Related Research 469, 2327–2336.

Moro, T., Kawaguchi, H., Ishihara, K., Kyomoto, M., Karita, T., Ito, H., Nakamura, K., Takatori, Y., 2009. Wear resistance of artificial hip joints with poly(2-methacryloyloxyethyl phosphorylcholine) grafted polyethylene: comparisons with the effect of polyethylene cross-linking and ceramic femoral heads. Biomaterials 30, 2995–3001.

Moro, T., Takatori, Y., Ishihara, K., Konno, T., Takigawa, Y., Matsushita, T., Chung, U.I., Nakamura, K., Kawaguchi, H., 2004. Surface grafting of artificial joints with a biocompatible polymer for preventing periprosthetic osteolysis. Nature Materials 3, 829–836.

Moro, T., Takatori, Y., Ishihara, K., Nakamura, K., Kawaguchi, H., 2006. 2006 Frank Stinchfield Award: grafting of biocompatible polymer for longevity of artificial hip joints. Clinical Orthopaedics and Related Research 453, 58–63.

Moro, T., Takatori, Y., Kyomoto, M., Ishihara, K., Saiga, K., Nakamura, K., Kawaguchi, H., 2010. Surface grafting of biocompatible phospholipid polymer MPC provides wear resistance of tibial polyethylene insert in artificial knee joints. Osteoarthritis Cartilage 18, 1174–1182.

Muratoglu, O.K., Bragdon, C.R., O'Connor, D.O., Jasty, M., Harris, W.H., 2001. A novel method of cross-linking ultra-high-molecular-weight polyethylene to improve wear, reduce oxidation, and retain mechanical properties. Recipient of the 1999 HAP Paul Award. Journal of Arthroplasty 16, 149–160.

Oral, E., Christensen, S.D., Malhi, A.S., Wannomae, K.K., Muratoglu, O.K., 2006. Wear resistance and mechanical properties of highly cross-linked, ultrahigh-molecular weight polyethylene doped with vitamin E. Journal of Arthroplasty 21, 580–591.

Palmer, R.R., Lewis, A.L., Kirkwood, L.C., Rose, S.F., Lloyd, A.W., Vick, T.A., Stratford, P.W., 2004. Biological evaluation and drug delivery application of cationically modified phospholipid polymers. Biomaterials 25, 4785–4796.

Paul, J.P., 1967. Forces transmitted by joints in the human body. Proceedings of the Institution of Mechanical Engineers 181, 8–15.

Selan, L., Palma, S., Scoarughi, G.L., Papa, R., Veeh, R., Di Clemente, D., Artini, M., 2009. Phosphorylcholine impairs susceptibility to biofilm formation of hydrogel contact lenses. American Journal of Ophthalmology 147, 134–139.

Shen, F.W., Lu, Z., McKellop, H.A., 2011. Wear versus thickness and other features of 5-Mrad crosslinked UHMWPE acetabular liners. Clinical Orthopaedics and Related Research 469, 395–404.

Snyder, T.A., Tsukui, H., Kihara, S., Akimoto, T., Litwak, K.N., Kameneva, M.V., Yamazaki, K., Wagner, W.R., 2007. Preclinical biocompatibility assessment of the EVAHEART ventricular assist device: coating comparison and platelet activation. Journal of Biomedical Materials Research Part A 81, 85–92.

Tipper, J.L., Galvin, A.L., Williams, S., McEwen, H.M., Stone, M.H., Ingham, E., Fisher, J., 2006. Isolation and characterization of UHMWPE wear particles down to ten nanometers in size from in vitro hip and knee joint simulators. Journal of Biomedical Materials Research Part A 78, 473–480.

Please cite this article as: Moro, T., et al., Grafting of poly(2-methacryloyloxyethyl phosphorylcholine) on polyethylene liner in artificial hip joints reduces production of wear particles. Journal of the Mechanical Behavior of Biomedical Materials (2013), http://dx.doi.org/10.1016/j.jmbbm.2013.03.011